Nanoscale Advances

ROYAL SOCIETY OF CHEMISTRY

PAPER

View Article Online
View Journal | View Issue

Cite this: *Nanoscale Adv.*, 2021, **3**, 5332

Synergizing Cu dimers and N atoms in graphene towards an active catalyst for hydrogen evolution reaction†

Jing Yang, Zhi Gen Yu and Yong-Wei Zhang *

Moving forward from single atom catalysts, here we propose Cu mers coordinated with N atoms in graphene as a potential catalyst for hydrogen evolution reaction (HER) using first-principles calculations. Our study shows that Cu mers (monomer, dimer and trimer) with no N coordination adsorb H too strongly, whereas Cu mers with complete N coordination adsorb H too weakly, indicating that neither is catalytically active for HER. However, these results imply that Cu mers with partial N coordination may exhibit a better catalytic performance. Thus, we further explored all the Cu_2N_x complexes with different atomic coordination numbers and spatial distributions and find that one of the Cu_2N_4 atomic configurations possesses a ΔG_{H*} of −0.09 eV, exhibiting a superior catalytic performance for HER. The possible reason might be that this configuration tunes the p-band center to an optimum level. Our study here reveals a promising catalyst for HER and presents a practical route to design catalysts by introducing metal mers and tuning their coordination with high-valence non-metal elements.

Received 22nd June 2021
Accepted 9th August 2021

DOI: 10.1039/d1na00469g

rsc.li/nanoscale-advances

1. Introduction

On the one hand, hydrogen evolution reaction (HER), which is perhaps the simplest way to produce high purity hydrogen, is highly desirable and of great importance for providing a viable solution to green energy and environmental sustainability.[1–3] On the other hand, HER may become undesirable and needs to be suppressed, for example, in the CO_2 reduction reaction (CO_2RR) and N_2 reduction.[4,5] Due to its unique role in electrochemistry, more studies should be devoted to understanding HER to either promote or suppress it.

To efficiently produce hydrogen, Pt-based materials, which possess a slightly negative hydrogen adsorption Gibbs free energy (ΔG_{H*}) and minimal overpotential, are considered the state-of-the-art electrocatalysts for HER.[6,7] However, the scarcity and high cost of Pt restrict these materials from widespread applications. After years of research, an active, stable and inexpensive alternative to Pt is still unavailable. Clearly, new design strategies for electrochemical catalysts are demanded to address this challenge.[8]

Single atom catalysts (SACs) recently emerged as a new frontier in electrocatalyst research. The underlying argument is that the dispersion of isolated metal atoms can maximize the efficiency of the metals, and thus may show excellent catalytic activities.[9–11] For example, SACs achieved by co-doping graphene with transition-metal (TM) and nitrogen (N) atoms (denoted as TM–N@graphene) exhibit a high electrochemical catalytic activity and thus were considered as promising substitutes for Pt-based electrocatalysts.[12–14] Importantly, these studies revealed that the synergy and coordination of TM atoms with neighboring N atoms play a crucial role in the catalytic activity of SACs.[15] This synergy was also supported by many other experimental and theoretical studies on TM–N@graphene SACs. For example, Guan *et al.* experimentally synthesized single atom Mn anchored in the N-doped graphene and reported its high performance for HER, and they ascribed the high activity to the coordination of N to Mn.[16] Chen *et al.* experimentally synthesized single atom Fe anchored in N-doped graphene, which gave high performance for the oxygen evolution reaction (OER) due to the dispersed highly catalytically active sites.[17] By using density functional theory (DFT), Wang *et al.* explored a series of single transition metals (Fe, Co, Ni, Cu, and Pd) anchored on various N-doped graphene as electrocatalysts for both HER and OER.[18] They revealed that Co with a triple-coordinated configuration exhibited a high catalytic activity toward HER and Co with a quadruple-coordinated configuration was a promising candidate for OER. Pennycook *et al.* demonstrated that atomically dispersed Ni with triple nitrogen coordination (Ni–N_3) on carbon could achieve an efficient HER performance in alkaline media and their DFT calculations verified that the Ni–N_3 coordination, which exhibited a lower coordination number than Ni–N_4, facilitated water dissociation and hydrogen adsorption, and hence enhanced the HER activity.[19]

*Institute of High Performance Computing, A*STAR, Singapore. E-mail: zhangyw@ihpc.a-star.edu.sg*

† Electronic supplementary information (ESI) available. See DOI: 10.1039/d1na00469g

Despite these extensive studies, an active, stable and inexpensive alternative to Pt-based electrocatalysts is still unavailable. However, the studies on SACs highlight the importance of synergy and coordination between the transition metal SACs and their neighboring nitrogen atoms in electrocatalytic activities and performance.[15,20] Based on the above, two interesting questions arise: if we extend a SAC to a cluster consisting a few metal atoms (or mer), what is its catalytic performance for HER? Can we leverage the synergetic effect between the metal mer and its neighboring N atoms to improve its catalytic performance for HER? To the best of our knowledge, although bi-metal catalysts with two adjacent copper atoms (Cu dimer) on Pd were synthesized and shown to carry out the critical bimolecular step in CO_2 reduction,[11] the Cu mers on graphene have not been experimentally synthesize before. Clearly, answers to these questions could provide a new route to design high-performance electrocatalysts for HER.

In this study, we propose Cu mers coordinated with N atoms in graphene, and explore their electrocatalytic performance for HER. Our first-principles calculations show that H adsorption energy in pure Cu mer catalysts (monomer, dimer and trimer anchored on graphene) without N embedding is too high while in the Cu mer catalysts with full N coordination is too low, suggesting that there may be an optimized coordination number that results in an optimum H Gibbs free energy and thus a better HER performance. Our comprehensive study indeed identifies a Cu_2N_4 atomic configuration that gives a ΔG_{H^*} of -0.09 eV, exhibiting superior catalytic performance for HER. Therefore, the present study shows that by extending the Cu SAC concept to the Cu mer catalyst concept, together with an optimum coordination number of N, one can obtain superior catalysts, which may outperform Pt-based electrocatalysts, and potentially present as an active, stable and inexpensive alternatives.

2. Computational details

The density functional theory (DFT) method implemented in the Vienna *Ab initio* Simulation Package (VASP) was used to study the HER electrocatalytic activities of Cu mer catalysts.[21,22] The Perdew–Burke–Ernzerhof functional under the generalized gradient approximation[23,24] was applied to mimic the exchange–correlation interaction. The cutoff kinetic energy was set to be 500 eV to expand the electronic wave functions. A gamma centered $3 \times 3 \times 1$ *k*-mesh was used for structural optimization.

The H adsorption energy (ΔE_{H^*}) is defined as:

$$\Delta E_{H^*} = E_{catalyst-H} - E_{catalyst} - 1/2E(H_2) \quad (1)$$

A positive ΔE_{H^*} indicates that the adsorption is not thermodynamically favorable while a negative ΔE_{H^*} indicates that the adsorption process is exothermic. Physically, the more negative the ΔE_{H^*} is, the stronger the adsorption is.

It is well believed that the first step of HER is the electrochemical hydrogen adsorption, often known as the Volmer reaction: $H^+ + e^- = H^*$. It is followed by either an electrochemical (Heyrovsky reaction: $H^* + H^+ + e^- = H_2$) and/or chemical (Tafel reaction: $H^* + H^* = H_2$) reaction to complete the entire HER process. Thus, the catalytic activity for the HER can be characterized by H Gibbs free energy:[25]

$$\Delta G_{H^*} = \Delta E_{H^*} + \Delta E_{ZPE} - T\Delta S_{H^*} \quad (2)$$

where $\Delta E_{H^*}$is the hydrogen adsorption energy obtained directly from DFT calculations. ΔE_{ZPE} is the difference in zero-point energy between the adsorbed hydrogen and the gas-phase hydrogen, and ΔS_{H^*} is the entropy difference between the adsorbed state and the gas phase. T is the room temperature at 298 K. Both ΔE_{ZPE} and ΔS_{H^*} can be calculated from vibrational frequencies of the system. ΔE_{ZPE} can be calculated from $\Delta E_{ZPE} = \Delta E_{ZPE}(H^*) - 1/2\Delta E_{ZPE}(H_2)$ obtained from the calculated vibrational frequencies of the adsorbed hydrogen.[26] ΔG_{H^*} is a key descriptor of the HER activity of the catalyst.[25] For an ideal catalyst, the Gibbs free energy value for the hydrogen adsorption on the catalyst should be close to 0 eV, that is, ΔG_{H^*} is close to 0. As we defined, a catalyst with a large positive ΔG_{H^*} value means the adsorption of H is too weak such that it is not kinetically favored for hydrogen adsorption. While a catalyst with a large negative ΔG_{H^*} value means that the adsorption of H is too strong and thus difficult to release the adsorbed hydrogen, causing poor HER activity.[27] The p-band center (εp) is defined as the energy with a width average value of the density of states (p) with respect to the Fermi level:

$$\varepsilon_p = \frac{\int_{-\infty}^{+\infty} n_p(\varepsilon)\varepsilon d\varepsilon}{\int_{-\infty}^{+\infty} n_p(\varepsilon) d\varepsilon} \quad (3)$$

where n_p and ε are projected-density of states (PDOS) and energy of p states. It is calculated with the code of VASPKIT.[28]

3. Results and discussions

Since the catalytic performance of Cu SACs is still not satisfactory,[29] we performed a comprehensive study on the catalytic performance of Cu mers coordinated with N atoms in graphene by identifying the most favorable hydrogen adsorption sites and calculating their respective ΔG_{H^*}. Before studying all possible cases, we first examined two extreme scenarios: pure Cu mer catalysts (monomer, dimer and trimer anchored on graphene) without N coordination, and Cu mers with full N coordination. It is expected that the results of these two extreme cases could provide valuable guidelines in designing high performance catalysts.

3.1 Cu mers with the lowest and highest N coordination number

The computational models of Cu monomer, dimer and trimer anchored on graphene (denoted as Cu_1N_0@graphene, Cu_2N_0@graphene and Cu_3N_0@graphene, respectively) are shown in the upper panel of Fig. 1. To study the impact of N, we built fully N atoms coordinated Cu monomer, dimer and trimer anchored on graphene (denoted as Cu_1N_4@graphene, Cu_2N_6@graphene and Cu_3N_8@graphene, respectively) shown in the lower panel of Fig. 1. The most stable Cu mer models obtained

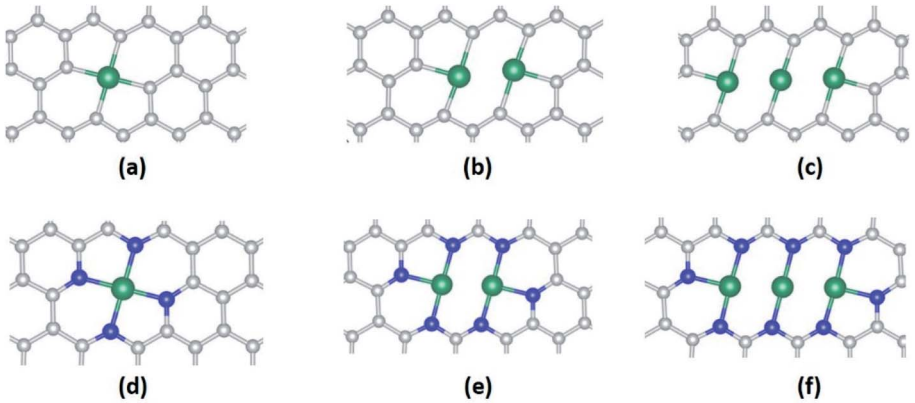

Fig. 1 Structure of (a) Cu_1N_0@graphene, (b) Cu_2N_0@graphene, (c) Cu_3N_0@graphene, (d) Cu_1N_4@graphene, (e) Cu_2N_6@graphene and (f) Cu_3N_8@graphene. Grey, navy and green spheres represent C, N and Cu atoms, respectively. The side view of these structures are summarized in Fig. S2.†

from our calculations are shown in Fig. 1. All the possible geometries and their relative formation energy are summarized in Fig. S1 and Table S1.† The ΔG_{H^*} for HER for these two sets of Cu mer catalysts (with the lowest and highest N concentration number) were calculated, and the results are summarized in Fig. 2. Without N atoms, the three Cu mer catalysts show a ΔG_{H^*} of −0.68 eV, −1.89 eV and −0.58 eV, respectively (the solid lines in Fig. 2). The negative ΔG_{H^*} values indicate that the catalysts adsorb the H too strongly. To achieve a better HER catalytic performance, we thus need to weaken the H Gibbs free energy. With full N coordination however, H adsorption by the Cu–N complexes varies dramatically: the Cu–N complexes show a ΔG_{H^*} of 0.49 eV, 0.42 eV and 0.38 eV, respectively (as show as the dot lines in Fig. 2). The positive ΔG_{H^*} values suggest that the catalysts adsorb H too weakly. These results are consistent with previous study on TM_1N_4@graphene SACs (TM = Co, Fe, Cu, Ni and Pd), which showed that these SACs were not able to effectively adsorb H due to the positive ΔG_{H^*}.[18] To achieve a better HER catalytic performance, we thus need to reduce ΔG_{H^*} in Cu–N complexes-based catalysts.

Clearly, at one extreme, Cu mer catalysts without N coordination (no N) adsorb H too strongly; while at the other extreme, the Cu mer catalysts with full N coordination adsorb H too weakly. Hence, it is expected that there would be an optimum coordination number of N atoms on Cu between the two extremes abovementioned that would result in an optimum ΔG_{H^*}, which may in turn lead to an excellent performance. Here, we focus on Cu dimer because the gap between Cu_2N_0@graphene and Cu_2N_6@graphene is the largest (Fig. 2), and hence, the Cu dimer is most suitable for demonstrating the synergic effect between Cu and N. Our reasoning is that if Cu dimer shows the synergetic effect, Cu monomer and Cu trimer should follow suit. To the best of our knowledge, it was reported that Cu dimer catalyst on Pd has been synthesized and reported promising catalytic performance for CO_2RR.[11] However, the study of N-coordinated Cu dimer catalyst for HER is still absent, which motivates us to perform comprehensive research on Cu dimer catalysts with all possible N coordination geometries to identify superior catalysts for HER.

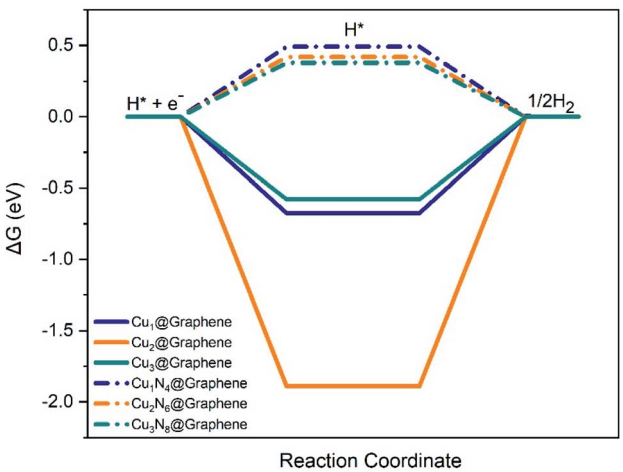

Fig. 2 ΔG_{H^*} diagram for HER on Cu monomer (navy), dimer (orange) and trimer (green) with highest (dot line) and lowest (solid line) N coordination number in graphene matrix.

3.2 Possible geometries of Cu_2N_x@graphene

Here, we aim to study Cu dimer catalysts with all possible N coordination geometries (with different numbers and arrangement of atoms). For Cu dimer on graphene, there can be up to 6 coordinated N atoms. In total, there are 22 possible Cu_2N_x complexes and the optimized geometries are summarized in Fig. 3. They all exhibit a 2D planar structure as shown in Fig. S2.†

For Cu_2@graphene (Fig. 3a), both Cu atoms prefer the double carbon vacancies, and the neighboring six C atoms form a stretched hexagon with the Cu atoms located in the middle of two C atoms and the C–Cu–C forms the long side of the hexagon. The calculated Cu–C bond length is 2.01 Å and bond angle of ∠C–Cu–Cu is 65.9°. Cu_2@graphene can host up to 6 N atoms, that is, Cu_2N_6@graphene (Fig. 3v). It keeps the stretched hexagon shape with a Cu–N bond length of 1.93 Å and ∠N–Cu–

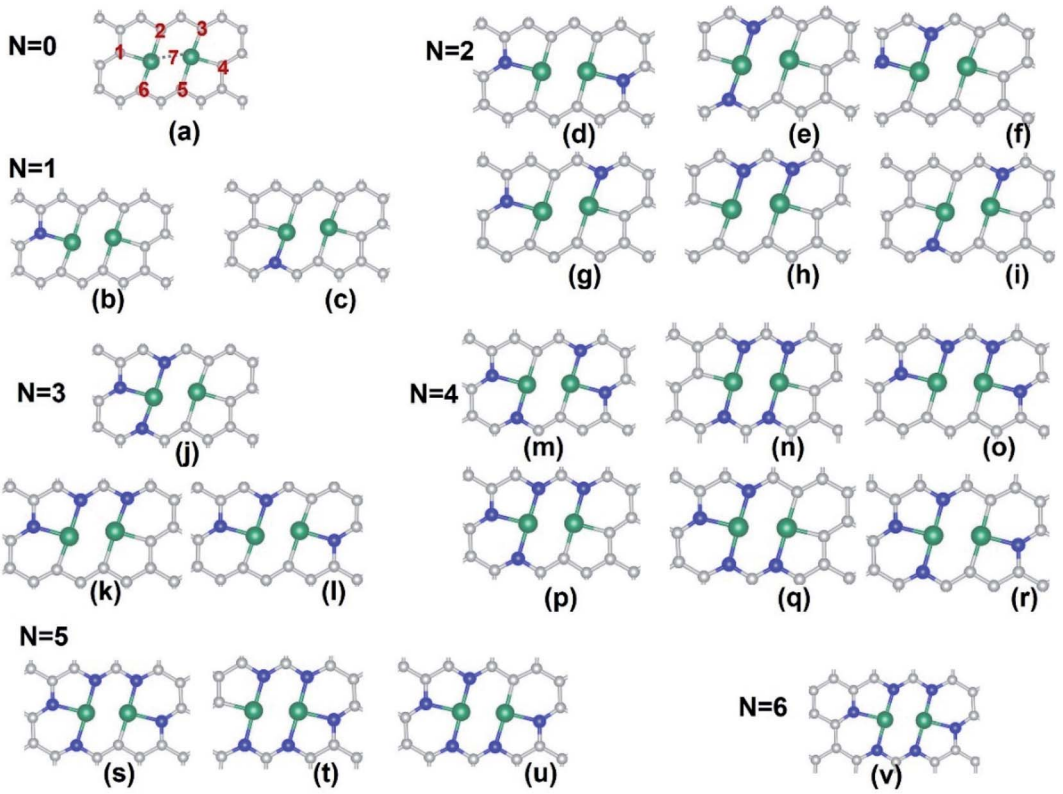

Fig. 3 All possible geometries of Cu_2N_x@graphene with $x = 0$ to 6. Grey, navy and green spheres represent C, N and Cu atoms, respectively. The number on (a) shows all the possible adsorption sites for H on top of Cu_2N_x@graphene with $x = 0$ to 6.

Cu of 75.2°. There are 2 possible geometries of Cu_2N_1@-graphene: N atom can either substitute the C atom next to Cu but not within the hexagon (Fig. 3b), or substitute the C atom next to Cu within the hexagon (Fig. 3c). Details of other possible Cu_2N_x@graphene can be found in Fig. 3.

3.3 Adsorption of H

The adsorption of protons onto the catalyst is the first step in HER. Therefore, we carefully examined all the possible adsorption sites for H, aiming to find the most favorable adsorption. It is then used to calculate ΔG_{H^*}, which is in turn used to estimate its catalytic performance for HER. The H may adsorb on top of either C, N or Cu sites. As shown in Fig. 3a, for each Cu_2N_x@graphene geometry, we tested all the 7 possible adsorption sites. The results are summarized in Table 1.

For Cu_2@graphene, H prefers adsorption onto the C at #2 site with strong chemical bonding and the ΔE_{H^*} is calculated to be −1.94 eV. The C–H bond is as long as 1.10 Å and C–H bond is not vertical to the graphene sheet but tilted to the neighboring Cu atom with a ∠H–C–Cu of 79.7°. Upon substituting the C at the #1 site with a N atom (Fig. 3b), the H prefers adsorption onto #3 site with an ΔE_{H^*} of −1.00 eV. On the other hand, if the N atom substitutes the C at #6 site (Fig. 3c), H prefers adsorption onto #2 site with an ΔE_{H^*} of −1.15 eV. Moving onto Cu_2N_2@graphene, there are 6 possible geometries. The strongest adsorption happens on the geometry in which the two N atoms substitute #2 and #6 sites (Fig. 3e), and the #1 site is the most favorable adsorption site with an adsorption energy as strong as −1.03 eV. The weakest stable H adsorption happens on top of geometry shown in Fig. 3g, in which the two N atoms substitute #1 and #3 sites, and the #4 site is the most favorable adsorption site with an adsorption energy as strong as −0.59 eV. There are 3 possible geometries for Cu_2N_3@graphene (Fig. 3j–l), which give a similar H adsorption energy from −0.63 to −0.74 eV, as shown in Table 1. Similar to Cu_2N_2@graphene, there are 6 possible geometries for Cu_2N_4@graphene. The strongest adsorption happens when the four N atoms substitute #1, #2, #4 and #6 sites (Fig. 3r), with #3 site being the most favorable adsorption site with an adsorption energy as strong as −0.76 eV. The weakest stable H adsorption happens on top of geometry p as shown in Fig. 3, in which the four N atoms substitute #1, #2, #3 and #6 sites (Fig. 3g), with #5 site being the most favorable adsorption site with an adsorption energy of −0.23 eV. There are 3 possible geometries for Cu_2N_5@graphene and the strongest H adsorption energy is up to −0.93 eV (Fig. 3t) and the weakest adsorption energy is −0.46 eV (Fig. 3s). When both Cu atoms are fully bonded to N atoms (Fig. 3v), the H prefers adsorption onto the Cu–Cu bridge site rather than the N site. However, the adsorption is not stable since the ΔE_{H^*} is 0.35 eV, indicating that the adsorption of H onto Cu_2N_6@graphene is not favorable.

3.4 H Gibbs free energy ΔG_{H^*}

After we identified the most favorable adsorption sites of H on various Cu_2N_x@graphene ($x = 0$ to 6) substrates, the most favorable adsorptions were used to calculate the ΔG_{H^*} diagram and we used the ΔG_{H^*} to estimate the catalytic performance of

Table 1 H adsorption energy (ΔE_{H^*}) at the most favorable site on top of Cu_2N_x@graphene with $x = 0$ to 6 (in eV)

# of N		ΔE_{H^*}	Position of N	Favorable site of H	# of N		ΔE_{H^*}	Position of N	Favorable site of H
$x = 0$	a	−1.94	NA	2	$x = 3$	l	−0.74	1, 2, 4	3
$x = 1$	b	−1.00	1	3	$x = 4$	m	−0.43	1, 3, 4, 6	2
	c	−1.15	2	2		n	−0.75	2, 3, 5, 6	1
$x = 2$	d	−0.68	1, 4	2		o	−0.64	1, 2, 3, 4	6
	e	−1.03	2, 6	1		p	−0.23	1, 2, 3, 6	5
	f	−0.75	1, 2	6		q	−0.41	1, 2, 5, 6	4
	g	−0.59	1, 3	4		r	−0.76	1, 2, 4, 6	3
	h	−0.75	2, 3	1	$x = 5$	s	−0.46	1, 2, 3, 4, 6	5
	i	−0.95	3, 6	4		t	−0.93	2, 3, 4, 5, 6	1
$x = 3$	j	−0.63	1, 2, 6	4		u	−0.62	1, 2, 4, 5, 6	3
	k	−0.71	1, 2, 3	4	$x = 6$	v	0.35	1, 2, 3, 4, 5, 6	7

these Cu_2N_x@graphene catalysts for HER. When the Cu atoms are fully bonded to N atoms, Cu_2N_6@graphene gives a ΔG_{H^*} of 0.42 eV (orange line in Fig. 4), which indicates that the adsorption of H on Cu_2N_6@graphene is energetically unfavorable. This is in line with the ΔE_{H^*} calculation that the ΔE_{H^*} on Cu_2N_6@graphene is 0.35 eV (Table 1). When the Cu atoms are fully bonded to C atoms, Cu_2@graphene gives a ΔG_{H^*} of −1.89 eV (grey line in Fig. 4), which indicates that the adsorption of H on Cu_2N_6@graphene is too strong. This is in line with the ΔE_{H^*} calculation that the ΔE_{H^*} of H on Cu_2@graphene is −1.94 eV (Table 1). For other geometries, the Cu and N atoms work together and the relative ΔG_{H^*} values are in between the two extreme cases above.

We noted that the Cu_2N_4@graphene with the p configuration gives a ΔG_{H^*} of −0.09 eV, which is very close to zero. Hence, it is expected that this atomic configuration can be a very active catalyst for HER. This is also in line with the ΔE_{H^*} calculations where amongst designs that give negative ΔG_{H^*}, Cu_2N_4@graphene with the p configuration shows an exothermic and yet weakest ΔE_{H^*} (−0.23 eV). Our result is also consistent with previous reports that TM–N@graphene SACs with the highest N coordination number demonstrate a poor HER performance as their interactions with H* are too weak, while a relatively lower N coordination number results in a better HER catalytic performance.[18,30]

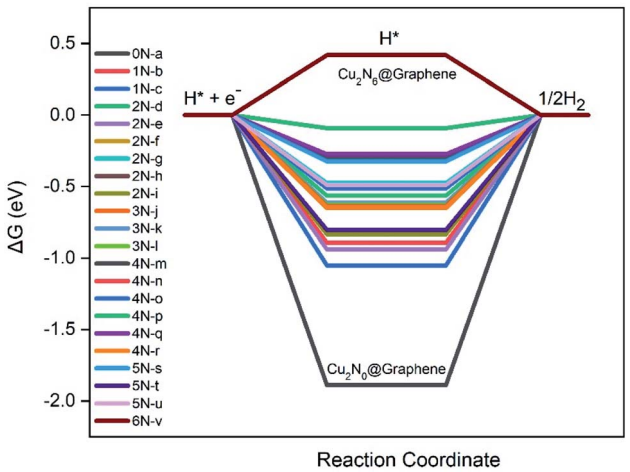

Fig. 4 ΔG_{H^*} diagram for HER on Cu_2N_x@graphene ($x = 0$ to 6) substrates.

3.5 Electronic structure analysis

To elucidate the synergistic effect that Cu dimer and N on graphene substrate have on the electronic structure and chemical properties, we calculated the atom-projected p-orbital density of states of the substrate, as summarized in Fig. 5. For Cu_2N_0@graphene, the p-band center with respect to the Fermi level is calculated to be at −5.09 eV. When the N coordination number increase, the p-band center moves downwards to −5.69 eV for Cu_2N_4@graphene (p configuration as shown in Fig. 3). The redshift of the p-band center suggests that the hybridization strength of substrate p-band and H-s orbital decreases, leading to a decrease in H adsorption energy.[31,32] The calculated p-band centers are consistent with the computed H adsorption

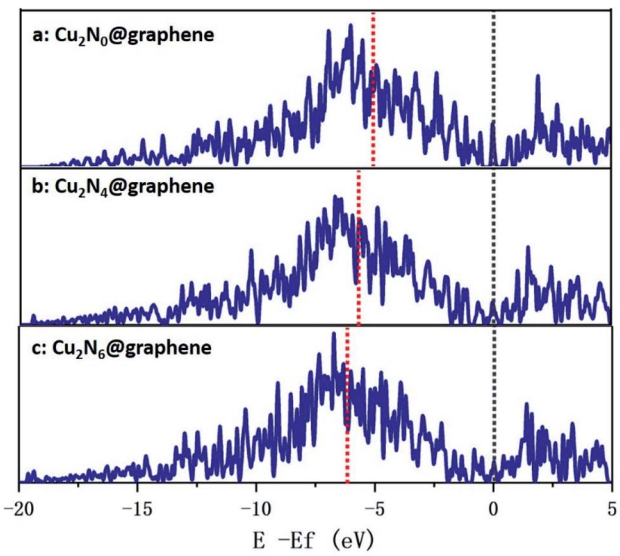

Fig. 5 Calculated PDOS of the p-band of the substrate (a) Cu_2N_0@graphene, (b) Cu_2N_4@graphene (p configuration as shown in Fig. 3) and (c) Cu_2N_6@graphene. The Fermi level is set at the zero of energy, and the p-band center is marked by the red dashed line.

energies, where the H adsorption weakens from −1.94 eV to −0.23 eV when the N coordination number increases from Cu_2N_0@graphene to Cu_2N_4@graphene. The p-band center of Cu_2N_6@graphene is further down shifted to −5.92, which might be responsible for its unfavorable adsorption ($\Delta E_{H^*} = +0.35$ eV). We further calculated the charge density difference map (Fig. S3†). For Cu_2N_6@graphene, the charge redistribution results in more antibonding states and fewer bonding states forming between the adsorbed H and host atoms, which might be responsible for its thermodynamically unfavorable adsorption. This suggests that the Cu_2N_4@graphene with p configuration (shown in Fig. 3) tunes the p-band center to the optimum level, which leads to an ideal H adsorption strength (the ΔG_{H^*} value of −0.09 eV).

4. Conclusion

We have systematically investigated the synergistic effect between the transition metal atoms and nitrogen atoms, and how they can tune the performance of Cu_2N_x@graphene catalysts. The highest N coordination number (with Cu binding to only N atoms) leads to too strong H adsorption, while the lowest N coordination number (with Cu binding to C atoms) leads to too weak H adsorption for catalyzing HER. It is expected that there may be an optimized N coordination number such that the Cu dimer and N atoms can cooperate to give the optimum H Gibbs free energy, which in turn provides us with a better catalyst for HER. We have studied all 22 possible Cu_2N_x@graphene geometries with different numbers and arrangements of N atoms to identify the configuration with the optimum ΔG_{H^*}. We find that Cu_2N_4@graphene with the p configuration exhibits a ΔG_{H^*} of −0.09 eV, which shows a remarkable improvement compared to the ones with the highest N coordination number (Cu_2N_6@graphene, $\Delta G_{H^*} = 0.42$ eV) and the lowest N coordination number (Cu_2N_0@graphene, $\Delta G_{H^*} = -1.89$ eV). Our results are in line with previous reports showing that TM–N@graphene SACs with the highest N coordination demonstrate a poor HER performance as their interactions with H* are too weak, while SACs with a relatively lower N coordination show a better HER catalytic performance.[18,30] By performing the PDOS calculations, we find that this configuration is able to tune the p-band center, which in turn leads to an optimum adsorption strength. The idea of introducing metal mers together with coordination number tuning may present a feasible route towards designing superior catalysts not just for HER, but beyond, for example, tackling CO_2RR, N_2 reduction reaction and OER.

Author contributions

Jing Yang: DFT calculations, data curation and writing – original draft. Zhi Gen Yu: writing – review & editing. Yong-Wei Zhang: conceptual design, review, editing, fund acquisition, supervision.

Conflicts of interest

The authors declare that they have no known competing financial interests or personal relationships that could have appeared to influence the work reported in this paper.

Acknowledgements

This work was supported by NRF-CRP24-2020-0002. The authors acknowledge the computing resources support from A*STAR Computational Resource Centre (A*CRC) and National Supercomputer Centre, Singapore (NSCC).

References

1 S. Dunn, *Int. J. Hydrogen Energy*, 2002, **27**, 235–264.
2 Z. Pu, I. S. Amiinu, Z. Kou, W. Li and S. Mu, *Angew. Chem., Int. Ed.*, 2017, **56**, 11559–11564.
3 B. Tang, J. Yang, Z. Kou, L. Xu, H. L. Seng, Y. Xie, A. D. Handoko, X. Liu, Z. W. Seh, H. Kawai, H. Gong and W. Yang, *Energy Storage Mater.*, 2019, **23**, 1–7.
4 C. Zhao, X. Dai, T. Yao, W. Chen, X. Wang, J. Wang, J. Yang, S. Wei, Y. Wu and Y. Li, *J. Am. Chem. Soc.*, 2017, **139**, 8078–8081.
5 Z. Geng, Y. Liu, X. Kong, P. Li, K. Li, Z. Liu, J. Du, M. Shu, R. Si and J. Zeng, *Adv. Mater.*, 2018, **30**, 1803498.
6 S. Bai, C. Wang, M. Deng, M. Gong, Y. Bai, J. Jiang and Y. Xiong, *Angew. Chem., Int. Ed.*, 2014, **53**, 12120–12124.
7 Y. Shiraishi, Y. Kofuji, S. Kanazawa, H. Sakamoto, S. Ichikawa, S. Tanaka and T. Hirai, *Chem. Commun.*, 2014, **50**, 15255–15258.
8 S. J. Gutić, A. S. Dobrota, E. Fako, N. V. Skorodumova, N. López and I. A. Pašti, *Catalysts*, 2020, **10**, 290.
9 C. Zhu, S. Fu, Q. Shi, D. Du and Y. Lin, *Angew. Chem., Int. Ed.*, 2017, **56**, 13944–13960.
10 X.-F. Yang, A. Wang, B. Qiao, J. Li, J. Liu and T. Zhang, *Acc. Chem. Res.*, 2013, **46**, 1740–1748.
11 J. Jiao, R. Lin, S. Liu, W.-C. Cheong, C. Zhang, Z. Chen, Y. Pan, J. Tang, K. Wu, S.-F. Hung, H. M. Chen, L. Zheng, Q. Lu, X. Yang, B. Xu, H. Xiao, J. Li, D. Wang, Q. Peng, C. Chen and Y. Li, *Nat. Chem.*, 2019, **11**, 222–228.
12 H. Fei, J. Dong, M. J. Arellano-Jiménez, G. Ye, N. Dong Kim, E. L. G. Samuel, Z. Peng, Z. Zhu, F. Qin, J. Bao, M. J. Yacaman, P. M. Ajayan, D. Chen and J. M. Tour, *Nat. Commun.*, 2015, **6**, 8668.
13 H. Xu, D. Cheng, D. Cao and X. C. Zeng, *Nat. Catal.*, 2018, **1**, 339–348.
14 L. Fan, P. F. Liu, X. Yan, L. Gu, Z. Z. Yang, H. G. Yang, S. Qiu and X. Yao, *Nat. Commun.*, 2016, **7**, 10667.
15 Z.-L. Wang, X.-F. Hao, Z. Jiang, X.-P. Sun, D. Xu, J. Wang, H.-X. Zhong, F.-L. Meng and X.-B. Zhang, *J. Am. Chem. Soc.*, 2015, **137**, 15070–15073.
16 J. Guan, Z. Duan, F. Zhang, S. D. Kelly, R. Si, M. Dupuis, Q. Huang, J. Q. Chen, C. Tang and C. Li, *Nat. Catal.*, 2018, **1**, 870–877.
17 P. Chen, T. Zhou, L. Xing, K. Xu, Y. Tong, H. Xie, L. Zhang, W. Yan, W. Chu, C. Wu and Y. Xie, *Angew. Chem., Int. Ed.*, 2017, **56**, 610–614.
18 Y. Zhou, G. Gao, Y. Li, W. Chu and L. W. Wang, *Phys. Chem. Chem. Phys.*, 2019, **21**, 3024–3032.
19 W. Zang, T. Sun, T. Yang, S. Xi, M. Waqar, Z. Kou, Z. Lyu, Y. P. Feng, J. Wang and S. J. Pennycook, *Adv. Mater.*, 2021, **33**, 2003846.

20 X. Liu, I. S. Amiinu, S. Liu, K. Cheng and S. Mu, *Nanoscale*, 2016, **8**, 13311–13320.
21 G. Kresse, *J. Non-Cryst. Solids*, 1995, **192–193**, 222–229.
22 G. Kresse and J. Hafner, *Phys. Rev. B*, 1993, **48**, 13115–13118.
23 J. P. Perdew, K. Burke and M. Ernzerhof, *Phys. Rev. Lett.*, 1996, **77**, 3865–3868.
24 P. E. Blöchl, *Phys. Rev. B*, 1994, **50**, 17953–17979.
25 J. K. Nørskov, T. Bligaard, A. Logadottir, J. R. Kitchin, J. G. Chen, S. Pandelov and U. Stimming, *J. Electrochem. Soc.*, 2005, **152**, J23.
26 C. Tsai, F. Abild-Pedersen and J. K. Nørskov, *Nano Lett.*, 2014, **14**, 1381–1387.
27 G. Rothenberg, *Catalysis: Concepts and Green Applications*, 2nd edn, 2017.
28 V. Wang, N. Xu, J.-C. Liu, G. Tang and W.-T. Geng, arXiv:1908.08269 2019.
29 H. Liu, X. Peng and X. Liu, *ChemElectroChem*, 2018, **5**, 2963–2974.
30 G. Gao, S. Bottle and A. Du, *Catal. Sci. Technol.*, 2018, **8**, 996–1001.
31 D. Liang, Y.-W. Zhang, P. Lu and Z. G. Yu, *Nanoscale*, 2019, **11**, 18329–18337.
32 A. M. Molenbroek, S. Helveg, H. Topsøe and B. S. Clausen, *Top. Catal.*, 2009, **52**, 1303–1311.